

# Probing of ultrasonic pulses by multidirectional light

K. Van Den Abeele\* and O. Leroy

K.U. Leuven Campus Kortrijk, Universitaire Campus, Interdisciplinary Research Center, B-8500 Kortrijk, Belgium

Received 12 February 1991

An acousto-optical reconstruction method for acoustic signals using multidirectional light diffraction by finite amplitude ultrasonic pulses is presented. When crossing the ultrasonic field, the far field diffracted laser light intensity of an incident convergent lightbeam becomes modulated in time. It is found that for special conditions, concerning direction of observation, ultrasonic frequency, power level and interaction length, the modulated light intensity is almost an exact copy of the diffracting acoustic pulse. Reconstruction can be completed by applying a fast Fourier transform (FFT) routine. Examples are provided and applications of this optical probing technique are suggested.

**Keywords:** acousto-optics; direct optical probing; ultrasonic characterization

As a result of the increasing interest in materials characterization, research concerning non-destructive testing (NDT) has made a lot of progress during the last few years. In several fields of research, it is widely known that ultrasound in combination with light provides an excellent measurement technique to investigate material properties<sup>1-5</sup>. Indeed, as an ultrasonic wave reacts to each change in the characteristics of the medium in which it propagates, its modification embodies every variation experienced during propagation. On the other hand, nobody can deny the fact that light is the most sensitive device with which to measure ultrasound, since the sound field is not disturbed by insertion of the measurement device.

Almost all modern theoretical studies concerning optical probing of ultrasonic waves have their origin in the work of Raman and Nath<sup>6</sup>, who explained the independent observations of Debey and Sears<sup>7</sup> and Lucas and Biquard<sup>8</sup> that an ultrasonic beam in liquid acts like a diffraction grating when illuminated by coherent light. Over the years the basic Raman-Nath theory has undergone many refinements and extensions, which has widened the scope of its applicability. Various models have been developed, supplying analytical and numerical expressions for the far field diffraction intensities due to the acousto-optic interaction of light with progressive<sup>9-11</sup>, standing<sup>12,13</sup>, superposed<sup>14-18</sup> or adjacent<sup>19-21</sup> ultrasonic waves at normal and oblique incidence. Further analysis of the analytical formulae in some specific cases explicitly shows that all information concerning the diffracting acoustic signal is contained in the far field light spectrum.

For adjacent ultrasonic waves with a frequency ratio of 1:2 or 1:4, for example, Leroy *et al.*<sup>20</sup> compared theoretical predictions of the relative ultrasonic amplitude with experimental observations. For finite amplitude low

frequency ultrasonic waves at normal incidence of light and small values of the pulse Raman-Nath parameter, Neighbors and Mayer<sup>17,22</sup> found that the individual diffraction orders provide a relative measure of the ultrasonic pulse's Fourier amplitude spectrum. Under the same circumstances, Nishida *et al.*<sup>23</sup> remarked that the amplitude of the diffraction pattern strongly depends on the phase relationship among the harmonic components of the ultrasonic wave. They proposed an inverse method to reconstruct, for an arbitrary cross-section, the original ultrasonic amplitude and phase spectrum by intensive calculations and they then applied it to investigate non-linearity properties of transparent media. Mayer *et al.*<sup>22,24</sup> and Wolf *et al.*<sup>25-27</sup> used the optical probing of pulses with parallel plane wave light to examine their harmonic growth due to medium non-linearities and their reflection and transmission on plates, simply by comparing the experimentally obtained diffraction patterns. Although theory and experiment seem to go hand in hand very well, it is not at present possible to deduce all the pertinent pulse characteristics from an evaluation of a light diffraction pattern and, as a consequence, it is not a straightforward matter to determine medium properties or plate characteristics using this traditional way of collecting information.

Other measurement techniques, such as the double beam illumination method<sup>28,29</sup> and near field models<sup>30-32</sup>, make use of the time dependence of the diffraction intensities for testing and investigating ultrasonically produced phase gratings. Such techniques have the advantage that they can even be applied in cases of very weak modulations, when the amount of light in the diffraction orders is comparable to the background noise caused by the scattered light. In the present paper we propose a direct acoustic pulsed signal reconstruction method based on Raman-Nath diffraction of multidirectional light. In this case, the far field diffraction

\* Aspirant of the Belgian National Foundation for Scientific Research

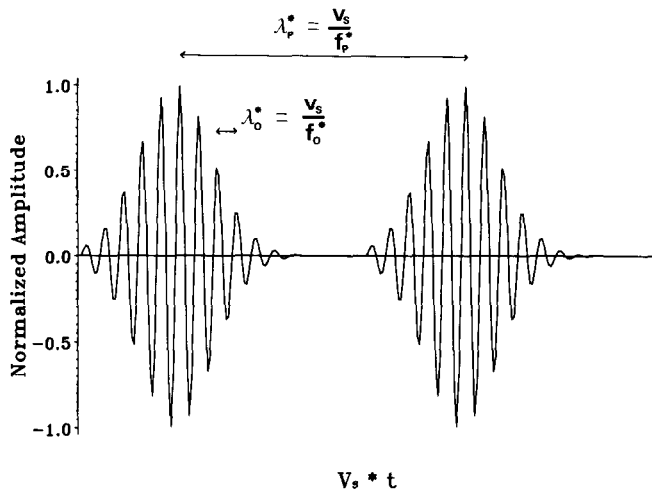


Figure 1 Illustration of repetition,  $f_r^*$ , and centre frequency  $f_o^*$ , for a typical pulse train. ( $v_s$  is the velocity of the sound in the medium)

intensities become time dependent and the modulation of the intensity in a specific direction behind the interaction cell is almost an exact copy of the diffracting pulse itself. A fast Fourier transform (FFT) of this time variation completes the reconstruction of the amplitude and phase spectra of the original acoustic signal at this cross-section. This direct visualization technique can be easily applied to investigate non-linear and absorption properties of transparent media or to examine characteristics of plates and layered materials through reflection and transmission. It is also useful for obtaining an immediate measurement of the frequency bandwidth of the mounted transducer.

**Theoretical set-up**

The time history of any arbitrary pulsed plane ultrasonic wave, as shown in Figure 1, can always be represented by a Fourier sine expansion, the pulse length corresponding to the repetition frequency,  $f_p^*$ , with centre frequency,  $f_o^* = \gamma \cdot f_p^*$  ( $\gamma \in \mathbb{N}$ ). As a consequence, and considering the chosen reference system (Figure 2), the distorted refractive index of the medium in which such a pulse train propagates can be expressed as follows

$$\mu(x, t) = \mu_0 + \mu \cdot \sum_{k=1}^K \alpha_k \sin\left(2\pi k \left(f_p^* t - \frac{x}{\lambda_p^*}\right) + \delta_k\right) \quad (1)$$

where;  $\mu_0$  is the refractive index of the non-perturbed medium;  $\mu$  is the largest variation; and  $\mu\alpha_k$  and  $\delta_k$  are the amplitude and phase of the  $k$ th Fourier component of the pulse.

From early work done by Raman and Nath<sup>6</sup> and many extensions of this study, we know that the intensity of a parallel beam of coherent light, with wavelength  $\lambda$  and frequency  $f$ , passing through such an acoustic grating at an angle of incidence  $\theta$ , splits into various diffracted orders, each of them undergoing different changes in amplitude, frequency and direction. Assuming that the ultrasonic waveform remains the same within the beamwidth of the light, the electric field of the  $r$ th component of the diffracted light, while crossing the

sound, can be written as

$$E_r(X, Z, t) = \Psi_r(\zeta) \exp(ira \sin \theta \zeta) \exp\left(-i \frac{2\pi}{\lambda} \mu_0 Z\right) \times \exp\left(2\pi ir X \frac{\cos \theta}{\lambda_p^*}\right) \exp[2\pi i(f - rf_p^*)t] \quad (2)$$

where

$$\begin{cases} X = x \cos \theta - z \sin \theta \\ Z = x \sin \theta + z \cos \theta \end{cases} \quad (3)$$

$$\zeta = \frac{2\pi}{\lambda} \mu Z \quad (4)$$

$$a = \frac{\lambda}{\mu \lambda_p^*} \quad (5)$$

$\Psi_r(\zeta)$  is the amplitude of the diffraction order satisfying the following system of differential equations

$$2 \frac{d\Psi_k}{d\zeta}(\zeta) - \sum_{j=1}^K \alpha_j [\Psi_{k-j}(\zeta) \exp(-i\delta_j) - \Psi_{k+j}(\zeta) \exp(i\delta_j)] = ik(k\rho_p - 2a \sin \theta) \Psi_k(\zeta) \quad (6a)$$

with boundary conditions

$$\Psi_k(\zeta = 0) = \delta_{k,0} \quad (k: -\infty \dots +\infty) \quad (6b)$$

and

$$\rho_p = \frac{\lambda^2}{\mu_0 \mu \lambda_p^{*2}} \cos^2 \theta \quad (7)$$

Comparing (2) with the general expression

$$A \exp\left[2\pi i \tilde{f} t - \frac{2\pi}{\lambda} i \mu_0 (X \sin \tilde{\theta} + Z \cos \tilde{\theta})\right]$$

for a plane electromagnetic wave in the medium, it is easily derived that the  $r$ th diffraction component experienced a frequency shift,  $-rf_p^*$ , and a change in direction with respect to the  $z$ -axis,  $\arcsin[-r(\lambda/\mu_0 \lambda_p^*) \cos \theta]$ .

Analytical and numerical expressions for the solutions  $\Psi_r(\zeta)$  of (6) can be obtained by many different methods for various cases<sup>14,15,17,18</sup>. As the amplitude functions depend only on space, the intensity,  $I_{-r} = E_r \cdot *E_r = \Psi_r \cdot * \Psi_r$ , of the diffraction spots at the observation plane in the far field are time independent. Such a typical far

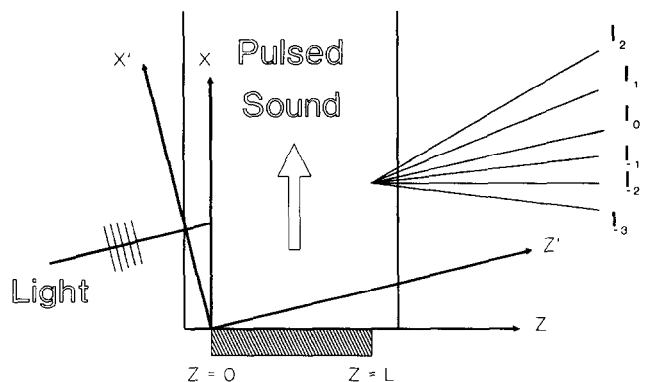
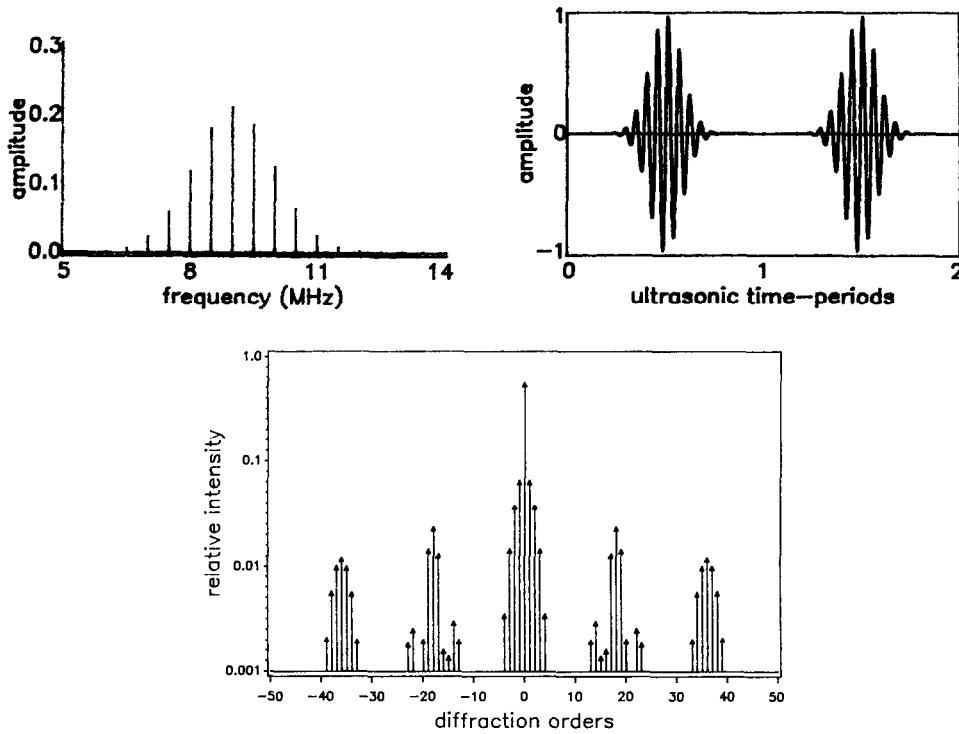


Figure 2 Schematic geometrical representation of the light diffraction process in the case of oblique incidence of parallel light on an arbitrary pulse train



**Figure 3** (a) Frequency spectrum (left) and amplitude distribution (right) of the pulsed ultrasound considered for the light diffraction pattern in part (b). (b) Typical far field light intensity diffraction pattern for parallel green argon laser light diffracted by pulsed ultrasound<sup>18</sup> at normal incidence (with logarithmic scale for the intensities)

field diffraction pattern for normal incidence of light is shown in Figure 3.

If we now consider multidirectional incident light of the same frequency, we must take into account the possibility of interfering diffraction orders behind the interaction cell. For far field measurements this interference only occurs for those diffracted light rays which have the same direction. Furthermore, as these diffracted orders originate from different incident light waves, they must have experienced different frequency shifts and consequently the intensity in this direction becomes time dependent.

In fact, as a first approximation, any incident convergent lightbeam may be seen as a multidirectional composition of parallel light with the same frequency and the same intensity. In the interests of the present study, we consider a convergent lightbeam incident between the angles  $M \cdot \beta$  and  $-N \cdot \beta$  [where  $\beta$  is the first Bragg angle,  $\lambda/(2\mu_0\lambda_p^*)$ ] and divide it into  $(M + N + 1)$  plane waves which are completely identical apart from their incidence direction  $[-N \cdot \beta, (-N + 1) \cdot \beta, (-N + 2) \cdot \beta, \dots, -\beta, 0, \beta, \dots, (M - 1) \cdot \beta, M \cdot \beta]$ . The  $n$ th component of this convergent optical beam ( $-N \leq n \leq M$ ), making an angle  $n \cdot \beta$  with respect to the normal, will diffract while crossing the sound. Its  $r$ th diffraction order then propagates within the medium in the direction

$$\frac{n\lambda}{2\mu_0\lambda_p^*} + \arcsin\left(-r \frac{\lambda}{\mu_0\lambda_p^*} \cos\left(\frac{n\lambda}{2\mu_0\lambda_p^*}\right)\right) \quad (8)$$

with respect to the normal ( $z$ -axis).

As  $\beta$  is very small in general ( $\approx 13 \times 10^{-5}$  rad at 1 MHz in water with green argon laser light), the angle of this diffraction order behind the interaction cell and outside the medium can be approximated by  $(n - 2r)$  [ $\lambda/(2\lambda_p^*)$ ]. The frequency shift of this diffracted ray is  $-rf_p^*$  and its amplitude,  $\Psi_r^{(n)}(\zeta^{(n)})$ , can be found by

solving (6) for  $\theta = \theta_{inc}^{(n)} = n\lambda/(2\mu_0\lambda_p^*) = n \cdot \beta$  and  $\rho_p \approx \lambda^2/(\mu_0\mu\lambda_p^{*2})$ .

The electric field for this  $(n, r)$  component can then be written as follows

$$\begin{aligned} E_r^{(n)}(X^{(n)}, Z^{(n)}, t) &= \Psi_r^{(n)}(\zeta^{(n)}) \\ &\times \exp\left[i \frac{2\pi}{\lambda} \mu_0 \left(r \frac{\lambda}{\mu_0\lambda_p^*}\right) X^{(n)} \cos \theta_{inc}^{(n)}\right] \\ &\times \exp\left[-i \frac{2\pi}{\lambda} \mu_0 \left(1 - r \frac{\lambda}{\mu_0\lambda_p^*} \sin \theta_{inc}^{(n)}\right) Z^{(n)}\right] \\ &\exp[2\pi i(f - rf_p^*)t] \end{aligned}$$

the superscript  $(n)$  referring to the angle of incidence  $n \cdot \beta$ . In terms of  $(x, z)$  coordinates, we find

$$\begin{aligned} E_r^{(n)}(x, z, t) &= \Psi_r^{(n)}(\zeta^{(n)}) \\ &\times \exp\left\{-i \frac{2\pi}{\lambda} \mu_0 \left[x \left(\sin \theta_{inc}^{(n)} - r \frac{\lambda}{\mu_0\lambda_p^*}\right) + z \cos \theta_{inc}^{(n)}\right]\right\} \\ &\times \exp[2\pi i(f - rf_p^*)t] \end{aligned} \quad (9)$$

with  $\zeta^{(n)} \approx (2\pi/\lambda)[\mu(z/\cos \theta_{inc}^{(n)})]$ .

As the  $r$ th diffraction order of the  $n$ th component of the incident converging beam only interferes with the  $s$ th order of the  $m$ th incident component if  $n - 2r = m - 2s$ , the total electric field in the direction  $k \cdot \beta$  can be expressed by

$$\begin{aligned} E_{(k)}^{total}(x, z, t) &= \sum_{r=r_1}^{r_2} \Psi_r^{(k+2r)}(\zeta^{(k+2r)}) \exp[2\pi i(f - rf_p^*)t] \\ &\times \exp\left\{-i \frac{2\pi}{\lambda} \mu_0 \left[x \left(\sin \theta_{inc}^{(k+2r)} - r \frac{\lambda}{\mu_0\lambda_p^*}\right) \right. \right. \\ &\left. \left. + z \cos \theta_{inc}^{(k+2r)}\right]\right\} \end{aligned}$$

where  $r_1$  is the smallest integer number larger than or equal to  $(-N - k)/2$  and  $r_2$  is the largest integer number smaller than or equal to  $(M - k)/2$ . The subscript  $(k)$  denotes the angle of observation  $k \cdot \beta$  behind the interaction cell. The intensity of the light propagating in this direction is directly proportional to the quantity

$$I_{(k)}(x, z, t) = E_{(k)}^{\text{total}}(x, z, t) \cdot *E_{(k)}^{\text{total}}(x, z, t)$$

the \* operation indicating complex conjugation.

Once the light has totally traversed the disturbed medium, its intensity is no longer affected by the sound wave. After some calculations we obtain that at  $z = L$  ( $L$  being the width of the transducer)

$$\begin{aligned} I_{(k)}(t) = & \sum_{r=r_1}^{r_2} \sum_{s=r_1}^{r_2} \Psi_r^{(k+2r)}(\zeta^{(k+2r)}|_{z=L}) \\ & \times * \Psi_s^{(k+2s)}(\zeta^{(k+2s)}|_{z=L}) \exp[2\pi i(s-r)f_p^* t \\ & + i \frac{2\pi}{\lambda} \mu_0 L (\cos \theta_{\text{inc}}^{(k+2s)} - \cos \theta_{\text{inc}}^{(k+2r)})] \end{aligned} \quad (10)$$

This expression, representing the far field intensity in the direction  $k \cdot \beta$  after diffraction of a convergent lightbeam incident between the angles  $M \cdot \beta$  and  $-N \cdot \beta$ , clearly illustrates the time modulation of the measured light intensity.

In order to investigate this time dependence more thoroughly, we made equation (10) explicit in the case of extreme Raman-Nath interaction, i.e. for rather small ultrasonic frequencies. However, it must be emphasized that the validity of this expression is not limited and thus can be used for Bragg conditions too.

The exact analytical solutions,  $\Psi_r^{(n)}(\zeta^{(n)}|_{z=L})$ , of system (6) for  $\theta = \theta_{\text{inc}}^{(n)}$  and  $\rho_p \approx 0$  are then given in the following form<sup>21</sup>

$$\begin{aligned} \Psi_r^{(n)}(\zeta^{(n)}|_{z=L}) = & \exp(-irbv^{(n)}) \sum_{q_2=-\infty}^{+\infty} \sum_{q_3=-\infty}^{+\infty} \cdots \sum_{q_K=-\infty}^{+\infty} \\ & J_{r-\sigma}(v_1^{(n)}) J_{q_2}(v_2^{(n)}) J_{q_3}(v_3^{(n)}) \cdots J_{q_K}(v_K^{(n)}) \\ & \times \exp \left[ -i \sum_{j=2}^K q_j \delta_j - i(r-\sigma)\delta_1 \right] \end{aligned} \quad (11)$$

with

$$\begin{aligned} b = \frac{1}{2} a \sin \theta_{\text{inc}}^{(n)} \quad a = \frac{\lambda}{\mu \lambda_p^*} \\ v^{(n)} = \frac{2\pi}{\lambda} \mu \frac{L}{\cos \theta_{\text{inc}}^{(n)}} \quad v_j^{(n)} \approx \alpha_j \frac{\sin(jbv^{(n)})}{jb} \quad j \in \{1 \cdots K\} \end{aligned}$$

and

$$\sigma = \sum_{j=2}^K jq_j$$

If we define

$$\Delta_{(k)}(m) = \frac{2\pi}{\lambda} \mu_0 L \cos \theta_{\text{inc}}^{(k+2m)} + \frac{\pi}{\lambda_p^*} L m \tan \theta_{\text{inc}}^{(k+2m)}$$

the total diffracted laser light intensity in the direction of observation,  $k \cdot \beta$ , takes on the form of the following

complicated, yet easily programmable, formula

$$\begin{aligned} I_{(k)}(t) = & \sum_{r=r_1}^{r_2} \sum_{q_2=-\infty}^{+\infty} \sum_{p_2=-\infty}^{+\infty} \cdots \sum_{q_K=-\infty}^{+\infty} \sum_{p_K=-\infty}^{+\infty} \\ & J_{r-\sigma}(v_1^{(k+2r)}) J_{r-\tau}(v_1^{(k+2r)}) J_{q_2}(v_2^{(k+2r)}) \\ & \times J_{p_2}(v_2^{(k+2r)}) \cdots J_{q_K}(v_K^{(k+2r)}) J_{p_K}(v_K^{(k+2r)}) \\ & \times \cos \left[ \sum_{j=2}^K (p_j - q_j) \delta_j - (\tau - \sigma) \delta_1 \right] \\ & + 2 \sum_{r=r_1}^{r_2} \sum_{s=r+1}^{r_2} \sum_{q_2=-\infty}^{+\infty} \sum_{p_2=-\infty}^{+\infty} \cdots \sum_{q_K=-\infty}^{+\infty} \sum_{p_K=-\infty}^{+\infty} \\ & J_{r-\sigma}(v_1^{(k+2r)}) J_{s-\tau}(v_1^{(k+2s)}) J_{q_2}(v_2^{(k+2r)}) \\ & \times J_{p_2}(v_2^{(k+2s)}) \cdots J_{q_K}(v_K^{(k+2r)}) J_{p_K}(v_K^{(k+2s)}) \\ & \times \cos \left[ 2\pi(s-r)f_p^* t + (s-r)\delta_1 - (\tau - \sigma)\delta_1 \right. \\ & \left. + \sum_{j=2}^K (p_j - q_j) \delta_j + \Delta_{(k)}(s) - \Delta_{(k)}(r) \right] \end{aligned} \quad (12)$$

where

$$\sigma = \sum_{j=2}^K jq_j$$

and

$$\tau = \sum_{j=2}^K jp_j$$

The first term in this expression is not time dependent. Its physical meaning is the summation of the intensities of the separated diffraction orders in this direction originating from the various components of the convergent lightbeam. The interference effects are all brought together in the second term which causes the time modulation.

In order to determine how the modulated light intensity initially develops, we can examine as a first approximation Equation (12) in the limit that all Raman-Nath parameters,  $v_r^{(n)}$ , are small, i.e. taking into account only those products of Bessel functions,  $J_{n_1} \cdot J_{n_2} \cdots J_{n_K} \cdot J_{m_1} \cdot J_{m_2} \cdots J_{m_K}$ , for which

$$\sum_{j=1}^K (|n_j| + |m_j|) \leq 1$$

This leads to a far more revealing expression

$$\begin{aligned} I_{(k)}(t) = & \prod_{i=1}^K J_0^2(v_i^{(k)}) + 2 \sum_{r=1}^{r_2} \prod_{i=1}^K [J_0(v_i^{(k)}) J_0(v_i^{(k+2r)})] \\ & \times \frac{J_1(v_r^{(k+2r)})}{J_0(v_r^{(k+2r)})} \cos[2\pi r f_p^* t + \delta_r + \Delta_{(k)}(r) - \Delta_{(k)}(0)] \\ & - 2 \sum_{r=1}^{-r_1} \prod_{i=1}^K [J_0(v_i^{(k)}) J_0(v_i^{(k-2r)})] \frac{J_1(v_r^{(k-2r)})}{J_0(v_r^{(k-2r)})} \\ & \times \cos[2\pi r f_p^* t + \delta_r + \Delta_{(k)}(0) - \Delta_{(k)}(-r)] \end{aligned}$$

As the angles of incidence are rather small, we can neglect their effect on the Raman-Nath parameters, so that  $\forall r, n, m \quad v_r^{(n)} = v_r^{(m)} = v_r = \alpha_r \cdot v = (2\pi/\lambda) \mu \alpha_r L$ . In this case, the laser light intensity in an arbitrary direction,

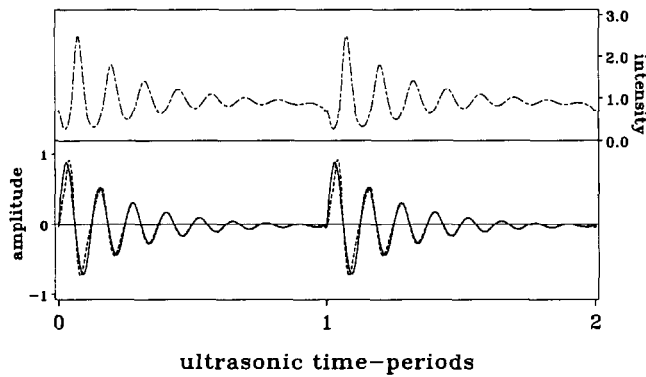


**Figure 4** Theoretical results of the presented model applied to an exponentially damped pulse ( $f_0 = 4$  MHz,  $f_p = 500$  kHz,  $\gamma = 8$ ,  $\nu = 1.6$ ) monitored by convergent green argon laser light ( $\lambda = 514$  nm). Upper curve: intensity of photodetector light as calculated by Equation (10). Lower curves: comparison of original acoustic signal (—) and reconstructed signal (---) obtained by FFT of the modulated light intensity shown in the upper curve. ( $\forall n \nu_n < 0.4$ )

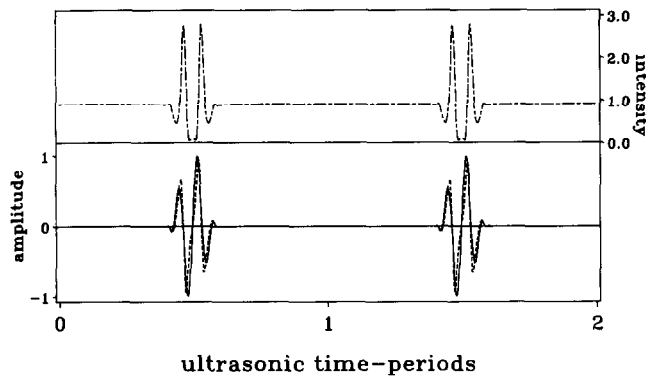


**Figure 5** Theoretical results of the presented model applied to a Gaussian-shaped pulse ( $f_0 = 2$  MHz,  $f_p = 142.8$  kHz,  $\gamma = 14$ ,  $\nu = 2.0$ ) monitored by convergent green argon laser light ( $\lambda = 514$  nm). Upper curve: intensity of photodetector light as calculated by Equation (10). Lower curves: comparison of original acoustic signal (—) and reconstructed signal (---) obtained by FFT of the modulated light intensity shown in the upper curve. ( $\forall n \nu_n < 0.25$ )

$k \cdot \beta$ , can be approximated by

$$I_{(k)}(t) = \prod_{i=1}^K J_0^2(v_i) \left\{ 1 + 2 \sum_{r=1}^{r_2} \frac{J_1(v_r)}{J_0(v_r)} \times \cos[2\pi r f_p^* t + \delta_r + \Delta_{(k)}(r) - \Delta_{(k)}(0)] - 2 \sum_{r=1}^{-r_1} \frac{J_1(v_r)}{J_0(v_r)} \cos[2\pi r f_p^* t + \delta_r - \Delta_{(k)}(-r) + \Delta_{(k)}(0)] \right\}$$

In the special case when we position a photodetector in the direction  $N \cdot \beta$  for a convergent lightbeam incident between the angles  $-N \cdot \beta$  and  $N \cdot \beta$  [ $r_1 = -N$ ,  $r_2 = 0$  and  $N$  being an integer value larger than the highest order Fourier component,  $K$ , needed in the representation of the pulse train (1)], we obtain

$$I_{(N)}(t) = \prod_{i=1}^K J_0^2(v_i) \left\{ 1 - 2 \sum_{r=1}^N \frac{J_1(v_r)}{J_0(v_r)} \times \cos[2\pi r f_p^* t + \delta_r - \Delta_{(N)}(-r) + \Delta_{(N)}(0)] \right\} \quad (13)$$

For values of  $\nu_r < 0.5$ ,  $r = 1 \dots N$  and  $2[J_1(v_r)/J_0(v_r)] \approx \nu_r$ , so that we may conclude that the modulation of this

measurable intensity in the first approximation contains all the information required to reconstruct the diffracting ultrasonic beam. Indeed, a fast Fourier transformation of (13) inevitably leads to a fairly good estimation for  $\nu_r$  and  $\delta_r$ ,  $r = 1 \dots N$ . Once these values are known the reconstruction of (1) is only a matter of some algebraic calculus [ $\mu \alpha_r = \nu_r(\lambda/2\pi L)$ ]. If  $\nu_r$  is larger than 0.5, one might obtain a better approximation by using a routine to invert the first order Bessel function as an intermediate step.

### Examples

To illustrate this reconstruction method we programmed the most general expression for the intensity in a specific direction, formula (10), with the amplitudes given by (11), which we calculated up to approximation level 3 (the sum, from  $j = 2$  to  $K$  of  $|q_j| + |r - \sigma| \leq 3$  for each amplitude). Starting from a known original acoustic pulse signal which causes a varying refractive index

$$\mu \cdot \sum_{k=1}^K \alpha_k \sin(2\pi k f_p^* t + \delta_k)$$

we calculate the modulation of the laser light intensity in the direction  $N \cdot \beta$  for an incident symmetrical convergent beam ( $-N \cdot \beta, N \cdot \beta$ ). A FFT routine attached to the program uses these results to obtain the approximated values for  $\nu_r$  and  $\delta_r$ , which we will call  $\nu_r^{FFT}$  and  $\delta_r^{FFT}$ . With these tabulated values a reconstructed signal has been drawn

$$\frac{\lambda}{2\pi L} \sum_{k=1}^K \nu_k^{FFT} \sin(2\pi k f_p^* t + \delta_k^{FFT})$$

( $f_p^*$  can be obtained experimentally from the separation of the far field diffraction spots in the case of normal incidence of plane parallel light.)

Figures 4–6 show some examples of this method for different pulses. In all illustrations 62 Fourier coefficients were used in the original signal and the value of  $N$  determining the width of the convergent beam and the direction of observation was  $\geq 62$ . The curve in the upper part of the figures corresponds to the results given by equation (10) for  $k = N$ ,  $r_1 = -N$  and  $r_2 = 0$ , and

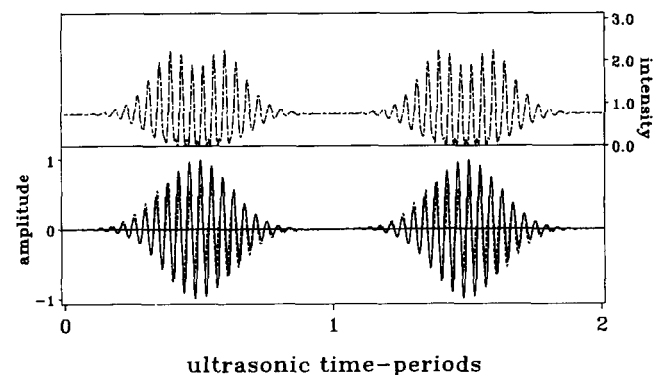


**Figure 6** Theoretical results of the presented model applied to a Gaussian-shaped pulse ( $f_0 = 2$  MHz,  $f_p = 83.3$  kHz,  $\gamma = 24$ ,  $\nu = 2.3$ ) monitored by convergent green argon laser light ( $\lambda = 514$  nm). Upper curve: intensity of photodetector light as calculated by Equation (10). Lower curves: comparison of original acoustic signal (—) and reconstructed signal (---) obtained by FFT of the modulated light intensity shown in the upper curve. (for  $n = 23, 24, 25$ ,  $\nu_n > 0.5$ )

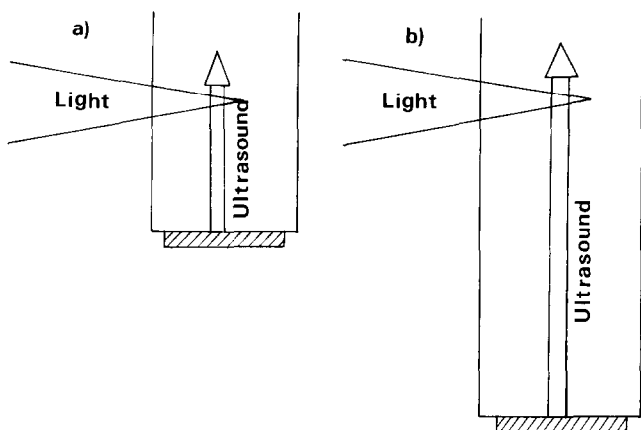


**Figure 7** Investigation of medium characteristics of optically transparent materials using pulsed ultrasound and convergent light. (a) Monitoring the soundbeam at a small distance from the transducer; (b) monitoring the soundbeam at a larger distance from the transducer

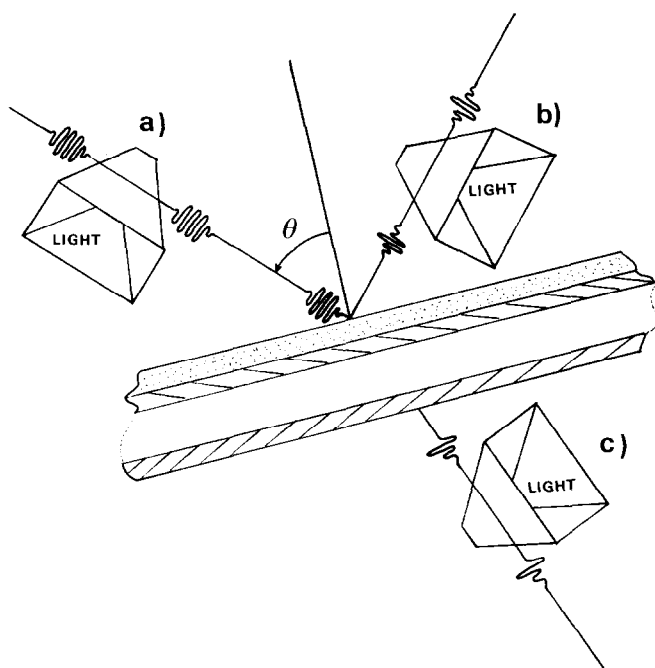


**Figure 8** Investigation of vibrational modes and material characteristics of layered media using reflection and transmission of ultrasonic pulses in combination with the direct optical probing technique. (a) Monitoring the incident soundbeam with convergent light; (b) monitoring the reflected soundbeam with convergent light; (c) monitoring the transmitted soundbeam with convergent light

represents the modulation in time of the photodetector intensity. The lower part compares the original signal (unbroken line) with the reconstructed one (dashed line), after normalization with respect to the peak amplitude of the original signal.

In cases when  $\forall r v_r < 0.5$  the comparison is almost impeccable (see Figures 4 and 5). If, for some integer values  $v_n > 0.5$ , the overall shape of the pulse can still be reconstructed, however, the agreement becomes poorer (Figure 6). As we suggested in the previous paragraph, an easy to use routine capable of inverting the first order Bessel function would improve the reconstruction. Other theoretical examples can be found in References 33 and 34.

### Applications for experimental research and conclusions

As already mentioned in the introduction, the utilization of light diffraction to characterize ultrasonic pulses and examine changes in the pulse spectrum due to medium non-linearities or due to reflection and transmission on layered materials has been widely proved and accepted. However, a full reconstruction of the diffracting pulse always necessitated lots of complicated manipulations and computations.

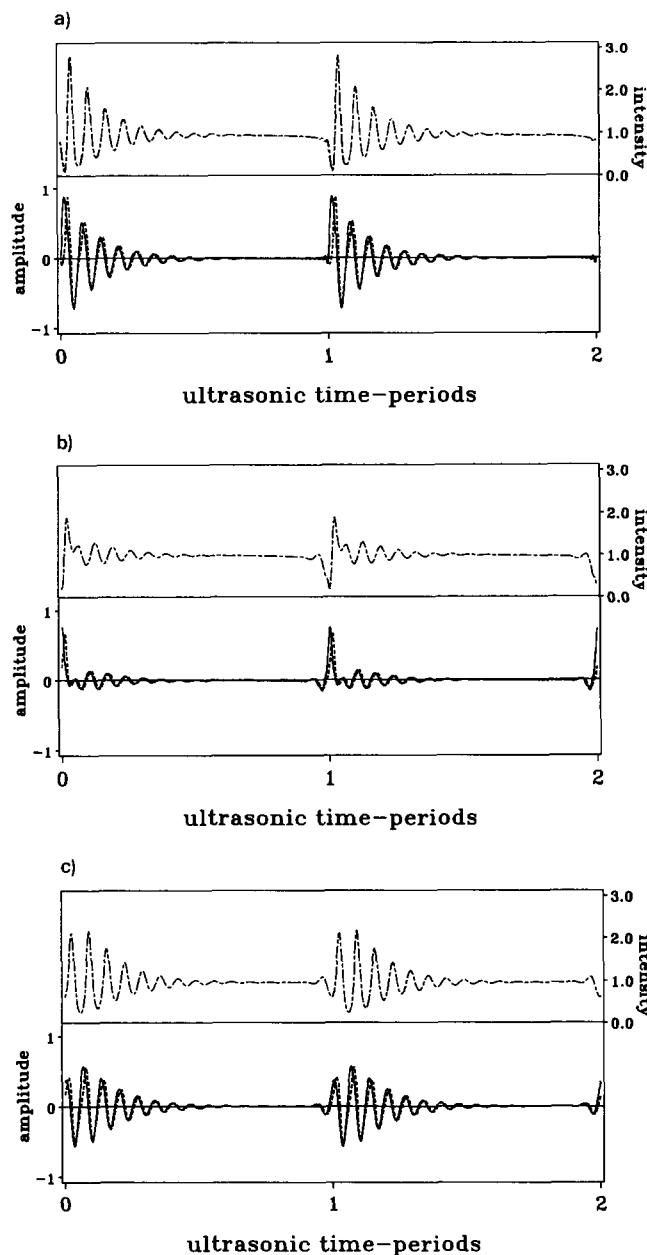


**Figure 9** Theoretical results of the suggested application to investigate reflection and transmission of ultrasonic pulses using convergent light. An incident exponentially damped pulse train ( $f_0 = 5.01$  MHz,  $f_p = 334$  kHz,  $\gamma = 15$ ,  $\nu = 2.0$ ) at  $30^\circ$  is reflected from and transmitted through a stainless steel plate of 1 mm thickness immersed in water. Incident (a), reflected (b) and transmitted (c) pulses can be directly reconstructed (---, lower part of each figure) from the photodetector light intensity (curve in upper part of each figure). Comparison of the reflected and transmitted spectra with the incident spectrum reveals interesting information concerning plate characteristics

In the present paper, we have shown that, using convergent light and a fast photodetector, visualization of acoustic signals is far from difficult. For low ultrasonic frequencies, low power and small interaction lengths, only a spectrum analyser, capable of performing a FFT of the measured light intensity in one specific direction, is needed to obtain a reliable picture of the pulsed ultrasonic wave. The simplicity of this model makes the method extremely suitable for investigation of ultrasound in many areas.

Medium non-linearities and absorption properties of optically transparent media can be visualized at once by monitoring the acoustic distorted medium at two different distances from the transducer with the same convergent lightbeam (Figure 7), or by performing the experiment twice at the same distance for different power levels of the ultrasonic wave<sup>35</sup>.

Polychromatic sound waves reflecting from and transmitted through layered media can be examined and compared with the incident sound wave (Figure 8), revealing vibrational modes and layer characteristics. Figure 9 illustrates this application for an exponentially damped pulse of 5.01 MHz centre frequency ( $f_0^* = 15 \cdot f_p^*$ ) incident at an angle of 30° on a stainless steel plate (1 mm) immersed in water. This figure clearly shows the effects of spectral filtering (see also Reference 34).

Even the presence and characteristics of surface waves at the boundary of two media, of which at least one is optically transparent, could be investigated by means of this direct optical probing technique.

Finally this method can be applied to transducer characterization. As the acoustic pulse spectrum originates from the discrete convolution of the ideal electrical input signal and the transfer curve of the transducer as a function of frequency, the reconstructed amplitude spectrum provides an immediate measurement of the frequency bandwidth of the transducer itself<sup>35</sup>.

## Acknowledgements

This work is supported by the National Foundation for Scientific Research of Belgium. The authors wish to thank Dr S.N. Antonov and Dr V.N. Sotnikov of the Institute of Radio Engineering and Electronics of the USSR Academy of Sciences, Moscow Region for their interest and the hopeful start of a series of experiments concerning this theoretical model.

## References

- 1 Cook, B.D. Determination of ultrasonic waveforms by optical methods *IEEE Trans Son Ultrason* (1964) **SU-11** 89–94
- 2 Korpel, A. *Acousto-optics in Applied Solid State Sciences* Vol 3 (Ed Wolfe, R.) Academic Press, New York, USA (1972) 71–180
- 3 Martin, F.D., Adler, L. and Brezazale, M.A. Bragg imaging with finite amplitude waves *J Appl Phys* (1972) **43**(4) 1480–1487
- 4 Reibold, R. and Molkenstruck, W. Light diffraction tomography applied to the investigation of ultrasonic fields. Part I: continuous waves *Acustica* (1984) **56** 181–192
- 5 Leroy, O. and Claeys, J.M. Acousto-optic method for nondestructive testing *J NDE* (1984) **4** 43–50
- 6 Raman, C.V. and Nath, N.S.N. The diffraction of light by sound waves of high frequency *Proc Ind Acad Sci* (1935) Part I **2** 406–412, Part II **2** 413–420, Part III **3** 75–84, Part IV **3** 119–125, Part V **3** 459–465
- 7 Debey, P. and Sears, F.W. On the scattering of light by supersonic waves *Proc Natl Acad Sci Washington* (1932) **18** 410–414
- 8 Lucas, R. and Biward, P. Propriétés optiques des milieux solides et liquides soumis aux vibrations élastiques ultrasonores *J Phys Radium* (1932) **3** 464–477
- 9 Phariseau, P. On the diffraction of light by progressive supersonic waves. Oblique incidence: Intensities in the neighborhood of the Bragg-angle *Proc Ind Acad Sci* (1956) **A44** 165–170
- 10 Kuliasko, F., Mertens, R. and Leroy, O. Diffraction of light by supersonic waves: the solution of Raman–Nath equations – I *Proc Ind Acad Sci* (1968) **67** 295–302
- 11 Blomme, E. and Leroy, O. Diffraction of light by ultrasound at oblique incidence: A MN-order approximation method *Acustica* (1987) **63** 83–89
- 12 Calligaris, F., Ciuti, P. and Gabrielli, I. Temporal light-modulation by two antiparallel soundbeams in thickscreen treatment *Acustica* (1977) **38** 37–43
- 13 Leroy, O. and Blomme, E. Amplitude–time modulation of a diffracted laser beam by two ultrasonic waves with opposite directions and frequency ratio 1:N *Acustica* (1984) **55** 224–232
- 14 Murty, J.S. Theoretical investigations of the diffraction of light by superposed ultrasonic waves *J Acoust Soc Am* (1954) **26** 970–974
- 15 Leroy, O. Theory of the diffraction of light by ultrasonic waves consisting of a fundamental tone and its n-1 harmonics *Ultrasonics* (1972) **10** 182–186
- 16 Häusler, E., Mayer, W.G. and Schwartz, M. Light diffraction by ultrasonic pulses *Acoust Lett* (1981) **4** 180–184
- 17 Neighbors, T.H. and Mayer, W.G. Asymmetric light diffraction by pulsed ultrasonic waves *J Acoust Soc Am* (1983) **74** 146–152
- 18 Van Den Abeele, K. and Leroy, O. Light diffraction by ultrasonic pulses: analytical and numerical solutions of the extended Raman–Nath equations *J Acoust Soc Am* (1990) **88** 2298–2315
- 19 Leroy, O. and Mertens, R. Diffraction of light by adjacent parallel ultrasonic waves with arbitrary frequencies (NOA-method) *Acustica* (1972) **26** 96–102
- 20 Leroy, O., Sliwinski, A., Kwiek, P. and Markiewicz, A. Diffraction of light by adjacent fundamental and second or fourth harmonic ultrasound beams: comparison of exact and simplified formulae with experiment *Ultrasonics* (1982) **20** 135–141
- 21 Blomme, E. Theoretical study of light diffraction by one or several ultrasonic waves in the MHz region *PhD Thesis* K.U. Leuven Campus Kortrijk, Belgium (1987)
- 22 Mayer, W.G. and Neighbors, T.H. Acousto-optic method for ultrasonic pulse characterization *Ultrasonics* (1987) **25** 83–86
- 23 Nishida, Y., Asada, I., Nakajima, M. and Yuta, S.I. Optical observation of finite amplitude ultrasonic fields *Electronics Commun Jpn* (1987) **70** (Part I, No. 5) 27–35
- 24 Mayer, W.G. and Neighbors, T.H. Optical probing of finite amplitude ultrasonic pulses *Proc 10th Int Symp Non-linear Acoustics* Kobe, Japan (1984) 113–116
- 25 Wolf, J., Neighbors, T.H. and Mayer, W.G. Optical probing of ultrasonic pulses *Ultrasonics* (1989) **27** 150–154
- 26 Wolf, J.W., Neighbors, T.H. and Mayer, W.G. Optical analysis of finite amplitude ultrasonic pulses *J Acoust Soc Am* (1990) **87** 1004–1009
- 27 Wolf, J.W., Neighbors, T.H. and Mayer, W.G. Spectral filtering of finite amplitude ultrasonic pulses by plates: an investigation using light diffraction *Acustica* (1990) **71** 93–99
- 28 Patorski, K. Diffraction testing of ultrasonically produced phase-gratings using a double beam illumination method *Ultrasonics* (1981) **19** 120–124
- 29 Leroy, O. and Blomme, E. Double Bragg and Bragg/normal diffraction of two laser beams by ultrasound *Ultrasonics* (1984) **22** 125–131
- 30 Cook, B.C. Measurement from the optical nearfield of an ultrasonically produced phase grating. *J Acoust Soc Am* (1976) **60** 95–99
- 31 Blomme, E., Briers, R. and Leroy, O. Reconstruction of a pulsed ultrasonic wave by light diffraction technique *Proc Seminar School: Acousto-Optics, Research and Developments* Leningrad, USSR (June–July 1990) in press
- 32 Blomme, E., Kwiek, P., Leroy, O. and Reibold, R. On the nearfield of light diffraction by an ultrasonic phase-amplitude grating: theory and experiment *Acustica* (1991) **73** 134–143
- 33 Van Den Abeele, K. and Leroy, O. Optical measurement of plane superposed ultrasonic waves *Proc IVth Spring School on Acousto-Optics and Applications* (Ed Sliwinski, A.) Gdansk, Poland (May 1989) 291–300
- 34 Van Den Abeele, K. and Leroy, O. Visualization of ultrasonic pulses by acousto-optic interaction with a conical lightbeam: farfield reconstruction method *Proc Seminar School: Acousto-Optics, Research and Developments* Leningrad, USSR (June–July 1990), in press
- 35 Antonov, S.N., Sotnikov, V.N., Leroy, O. and Van Den Abeele, K. Direct optical characterization of ultrasonic waves using Raman–Nath diffraction of convergent light *Ultrasonics* **29** 366–369